

Localized sp–d exchange interaction in ferromagnetic $\text{Ga}_{1-x}\text{Mn}_x\text{As}$ observed by magnetic circular dichroism spectroscopy of L critical points

This content has been downloaded from IOPscience. Please scroll down to see the full text.

2014 J. Phys. D: Appl. Phys. 47 355001

(<http://iopscience.iop.org/0022-3727/47/35/355001>)

View [the table of contents for this issue](#), or go to the [journal homepage](#) for more

Download details:

IP Address: 150.29.211.92

This content was downloaded on 08/08/2014 at 03:34

Please note that [terms and conditions apply](#).

Localized sp - d exchange interaction in ferromagnetic $\text{Ga}_{1-x}\text{Mn}_x\text{As}$ observed by magnetic circular dichroism spectroscopy of L critical points

H Tanaka¹, W M Jadwisienczak¹, H Saito², V Zayets², S Yuasa² and K Ando²

¹ Ohio University, School of Electrical Engineering and Computer Science, Athens, OH, 45701, USA

² National Institute of Advanced Industrial Science and Technology (AIST), Tsukuba, Ibaraki 305-8568, Japan

E-mail: ht287002@ohio.edu

Received 14 March 2014, revised 23 June 2014

Accepted for publication 24 June 2014

Published 7 August 2014

Abstract

We have conducted systematic investigations of magnetic circular dichroism (MCD) spectra and optical absorption spectra of the III-V diluted magnetic semiconductor (DMS) $\text{Ga}_{1-x}\text{Mn}_x\text{As}$. With an increase in Mn concentration x , the MCD structure originating from the L -critical points of the zinc-blend type band structure shifted towards lower energy while the corresponding absorption spectrum did not show the shift although they are expected to show the same dependence. This indicates that the s , p - d exchange interaction of $\text{Ga}_{1-x}\text{Mn}_x\text{As}$ has a very localized nature, because MCD is only active in a region where band structure is affected by Mn spins, and optical absorption results from the overall sample response. The MCD spectrum of a ferromagnetic $\text{Ga}_{0.97}\text{Mn}_{0.03}\text{As}$ sample was decomposed into contributions from Γ -critical points (E_0 and $E_0 + \Delta_0$), L -critical points (E_1 and $E_1 + \Delta_1$), and impurity band-related optical transitions. Using the intensities of MCD and optical absorption, the Zeeman splitting energy at E_1 was estimated to be larger than +8 meV at 6 K. By assuming the same ratio between the Zeeman splitting energies at E_0 and E_1 , which is experimentally reported in a II-VI paramagnetic DMS $\text{Cd}_{1-x}\text{Mn}_x\text{Te}$, the Zeeman splitting at E_0 of $\text{Ga}_{0.97}\text{Mn}_{0.03}\text{As}$ was estimated to be larger than +120 meV at 6 K.

Keywords: GaMnAs, Zeeman splitting, magnetic circular dichroism

(Some figures may appear in colour only in the online journal)

1. Introduction

$\text{Ga}_{1-x}\text{Mn}_x\text{As}$ is considered a prototype ferromagnetic diluted magnetic semiconductor (DMS) [1, 2]. However, there is no consensus regarding the electronic structure of $\text{Ga}_{1-x}\text{Mn}_x\text{As}$, and it is still under heated debate [3–12]. Since the most prominent characteristic of DMSs is the s , p - d exchange interactions between d -electron spins of magnetic ions and s , p carriers of the host material [13, 14], the most important task to clarify the electronic structure is the characterization of the spin-dependent band structure induced by the s , p - d exchange

interaction. Magnetic circular dichroism (MCD) spectroscopy is the most powerful tool utilized so far for this kind of study because it is very sensitive to the Zeeman splitting of the band structure that is a direct consequence of the s , p - d exchange interaction [14]. MCD spectroscopy has been successively used to clarify the electronic structures of II-VI DMSs [16–22], and it has been also applied to $\text{Ga}_{1-x}\text{Mn}_x\text{As}$ [10, 23–28]. However, the interpretation of the observed MCD spectra of $\text{Ga}_{1-x}\text{Mn}_x\text{As}$ itself has not reached conclusive consensus yet.

Using reflection mode MCD spectroscopy, Ando *et al* [23] came to the conclusion that the zinc-blend type semiconductor

band structure of $\text{Ga}_{1-x}\text{Mn}_x\text{As}$ is affected by Mn spin. They observed a negative MCD peak on a large positive MCD background signal that appeared at 1.52 eV and which corresponds to the E_0 band gap optical transition of host GaAs. The observed negative polarity suggested an antiferromagnetic nature of the p–d exchange interaction. In contrast, Szczyto *et al* [29] used transmission Zeeman spectroscopy to find that the broad absorption edge near the E_0 optical transition showed Zeeman splitting which corresponds to ferromagnetic p–d exchange interaction. In their analysis, only a contribution from the E_0 optical transition was assumed, as commonly adopted for the traditional magneto-optical analyses of paramagnetic II–VI DMSs. No magneto-optical background was taken into account. However, later studies showed that the most striking difference between the MCD spectra of II–VI DMSs and ferromagnetic $\text{Ga}_{1-x}\text{Mn}_x\text{As}$ is the respective absence and presence of a strong positive MCD background [23, 24, 26]. Using transmission mode MCD spectroscopy, Beschoten *et al* [24] noticed a large positive MCD background. However, as they described, the origin and spectral shape of the observed positive MCD background were not identified. By normalizing the MCD spectrum with its peak value without showing a clear justification of the normalization, they claimed to decompose the MCD spectrum into a positive unknown background and a negative peak which seems to reflect the antiferromagnetic p–d exchange interaction. However, the decomposed negative MCD peak appeared at 1.60 eV which was apparently higher than E_0 energy (1.52 eV) of host GaAs, and the positive and negative MCD components showed different temperature dependences. Such puzzling phenomena raise questions on the justification of the analytical methodology.

These confusions in the interpretation of the observed anomalous MCD spectra of ferromagnetic $\text{Ga}_{1-x}\text{Mn}_x\text{As}$ was solved later by MCD spectroscopy conducted in a much wider energy range, i.e. from 0.6 to 4 eV [26]. Ando *et al* found a large positive MCD peak around 1 eV. This impurity band (IB)-related MCD peak accompanies a broad positive MCD background tail on its higher energy side. It changes the apparent MCD polarity around E_0 from negative to positive. This strong influence of MCD background makes the interpretation of MCD spectra of $\text{Ga}_{1-x}\text{Mn}_x\text{As}$ very difficult, especially near the Γ -critical point (CP) [26]. In contrast, L -CPs, which are far away from the IB-related optical transitions, seem to be less affected. Therefore, one can expect to clarify the Zeeman splitting of $\text{Ga}_{1-x}\text{Mn}_x\text{As}$ at L -CP.

In this work, we conducted systematic investigations of the MCD and optical absorption spectra as a function of Mn concentration in $\text{Ga}_{1-x}\text{Mn}_x\text{As}$ to clarify the Zeeman splitting at L -CPs. Furthermore, we estimated Zeeman splitting energy at Γ -CP using a reported ratio [16–18] of Zeeman splitting between L -CP and Γ -CP of a II–VI DMS: $\text{Cd}_{1-x}\text{Mn}_x\text{Te}$.

2. Experimental procedure

$\text{Ga}_{1-x}\text{Mn}_x\text{As}$ thin films with (1 1 1)-orientation were grown on sapphire (000 1) substrates by molecular beam epitaxy (MBE). GaAs films were grown at both 600 °C (HT-GaAs)

and 230 °C (LT-GaAs), whereas $\text{Ga}_{1-x}\text{Mn}_x\text{As}$ thin films were grown at 230 °C. The film thickness was 50 nm in order to avoid optical interference effects. The Mn concentration of $x = 0.03$ sample was determined from x-ray photoelectron spectroscopy (XPS), calibrated by electron probe micro-analysis (EPMA). For the other films with smaller Mn content, x values were obtained from a calibrated relation between the amount of Mn beam flux and Mn Knudsen cell temperature, monitored in the growth chamber. The magnetization curves were measured by a superconducting quantum interface device (SQUID). Both MCD and optical absorption spectra were simultaneously measured in transmission mode using a Xe lamp. Magnetic field was applied parallel to the light propagation direction [14]. The incident light was modulated by a 50 kHz photoelastic modulator to right circularly polarized (RCP) and left circularly polarized (LCP) light. The sample area illuminated by light was about 5 mm². The absorption difference between RCP and LCP light, i.e. MCD, was detected by a lock-in amplifier. The 0.1 degree of MCD corresponds to 0.7% difference of optical absorption for RCP and LCP light [14]. Under an assumption that the Zeeman splitting ΔE of the electronic band structure causes the energy shift of the optical absorption spectrum for RCP and LCP light without changing the spectral shape (rigid band shift model), the MCD can be expressed as [14, 30, 31]

$$\text{MCD} = -\frac{45}{\pi} \Delta E \frac{dkL}{dE} \quad (1)$$

$$\Delta E = -g_{\text{eff}} \mu_B H \quad (2)$$

where k is the absorption coefficient, E is the photon energy, L is the sample thickness, g_{eff} is the effective g -value, μ_B is the Bohr magneton and H is the magnetic field. This rigid band shift model should be applicable for the L critical points of $\text{Ga}_{1-x}\text{Mn}_x\text{As}$, which are far away from the Fermi level. Zeeman splitting energy can be estimated by equation (1) by direct comparison between experimentally measured MCD and dkL/dE spectra.

3. Results

Figures 1(a)–(h) show MCD spectra of $\text{Ga}_{x-1}\text{Mn}_x\text{As}$ with different Mn concentrations as a function of photon energy measured at 6 K and 1 T. Magnetic field dependence of MCD intensity at 3.04 eV (figure 1(i)) shows that $\text{Ga}_{1-x}\text{Mn}_x\text{As}$ ($x = 0.03$) is ferromagnetic whereas samples with lower Mn concentrations are paramagnetic at 6 K. An inset in figure 1(i) shows that the normalized hysteresis loops measured by both MCD and SQUID are compatible with each other. Curie temperature T_c of $\text{Ga}_{1-x}\text{Mn}_x\text{As}$ ($x = 0.03$) determined from the Arrott plot of MCD intensity at different photon energies was 20 ± 2 K. These experimental results show that all the measured MCD spectra originate from $\text{Ga}_{1-x}\text{Mn}_x\text{As}$ [15, 26], and are free from other second-phase materials (e.g. small cluster of MnAs precipitations).

The MCD spectra show prominent characteristics around photon energies corresponding to Γ (E_0 and $E_0 + \Delta_0$) and L (E_1 and $E_1 + \Delta_1$) CPs of GaAs (figures 1(a)–(h)) [32].

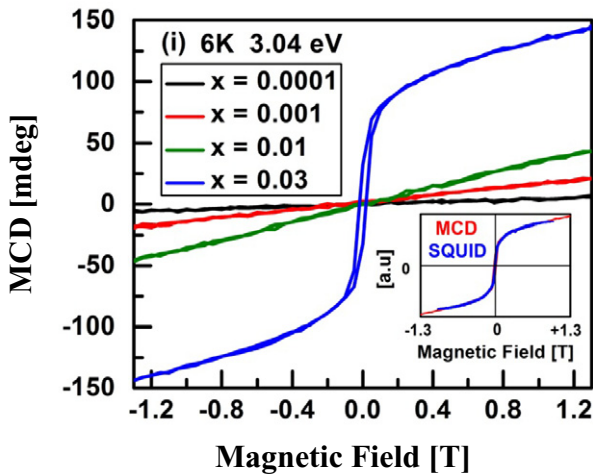
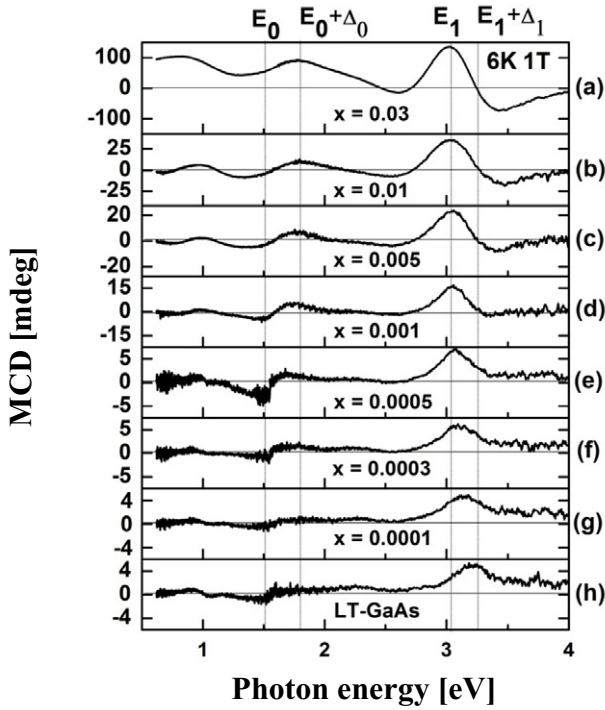


Figure 1. (a)–(h) MCD spectra of $\text{Ga}_{1-x}\text{Mn}_x\text{As}$ with different Mn concentrations at 6 K and 1 T as a function of photon energy. Photon energies corresponding to Γ (E_0 and $E_0 + \Delta_0$) and L (E_1 and $E_1 + \Delta_1$) CPs of GaAs are shown by vertical dotted lines. $\text{Ga}_{1-x}\text{Mn}_x\text{As}$ ($x = 0.03$) is ferromagnetic whereas samples with lower Mn concentrations are paramagnetic at 6 K. (i) Hysteresis loops of $\text{Ga}_{1-x}\text{Mn}_x\text{As}$ with different Mn concentrations at 3.04 eV and 6 K as a function of applied magnetic field. Inset shows normalized hysteresis loops measured by MCD and SQUID at 6 K between -1.3 and 1.3 T.

Around Γ -CPs, a pair of downward broad peak near E_0 and upward broad peak near $E_0 + \Delta_0$ is observed. It can be seen that the MCD spectral structure of ferromagnetic $\text{Ga}_{1-x}\text{Mn}_x\text{As}$ ($x = 0.03$) around E_0 is positive downward broad peak (figure 1(a)), whereas paramagnetic $\text{Ga}_{1-x}\text{Mn}_x\text{As}$'s ($x = 0.0001$ to 0.01) with smaller Mn concentration show negative downward broad peak (figures 1(b)–(h)). In addition, all samples show positive upward broad MCD peaks around $E_0 + \Delta_0$.

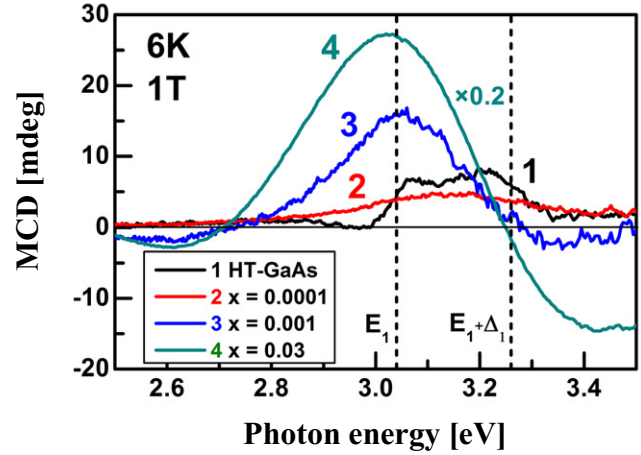


Figure 2. MCD spectra of HT-GaAs and $\text{Ga}_{1-x}\text{Mn}_x\text{As}$ with different Mn concentrations at 6 K and 1 T as a function of photon energy. Spectrum for $x = 0.03$ is multiplied by 0.2.

In MCD spectra of $\text{Ga}_{1-x}\text{Mn}_x\text{As}$ with lower Mn concentration (figures 1(e)–(h)), there are two upward peaks around 1 eV, which are below the band gap energy of the GaAs host (1.52 eV). It was observed that, those two peaks mix up and become one broad peak around 1 eV when Mn concentration becomes greater than $x = 0.001$ as seen in figure 1(d). The MCD spectra around 1 eV are due to contributions from multiple IB-related optical transitions [26]. Eventually, these IB-related MCD spectra become a broad peak with a long positive tail on the higher energy side, which acts as a very broad positive background for the MCD spectrum around E_0 and $E_0 + \Delta_0$. Furthermore, around L -CPs (E_1 and $E_1 + \Delta_1$), one broad positive peak is observed for each sample, and its magnitude increases with Mn concentration.

Figure 2 shows MCD spectra around L -CPs of HT-GaAs and $\text{Ga}_{1-x}\text{Mn}_x\text{As}$ with different Mn concentrations at 6 K and 1 T. The MCD spectrum of HT-GaAs clearly shows that it is composed of two dispersion-like structures with opposite polarities centred at E_1 and $E_1 + \Delta_1$ respectively. This indicates that the broad positive MCD peak around L -CP observed in LT-GaAs (figure 1(h)) resulted from the merging of these two dispersion-like MCD structures. The low temperature growth and Mn doping inevitably degrade the crystal structure quality of $\text{Ga}_{1-x}\text{Mn}_x\text{As}$, and cause the broadening of the MCD structures. Furthermore, figure 2 also shows that the broad positive MCD peak around L -CPs shifts its peak position to lower energy with increase in Mn concentration, and the shift seems to saturate with very small Mn concentration.

Figure 3(a) shows MCD and energy derivative of optical absorption (dkL/dE) spectra of HT-GaAs [33]. In both MCD and dkL/dE spectra, there are two dispersion-like structures centred at E_1 and $E_1 + \Delta_1$, respectively. Optical transitions at L -CPs of GaAs [34] are known to have a characteristic of the two-dimensional M_1 -type Van Hove singularity which should result in dispersion-like dkL/dE spectral shape at E_1 and $E_1 + \Delta_1$. The observed dispersion-like dkL/dE peaks in figure 3(a) is compatible with the theoretical expectation. It should be noted that a good correspondence between MCD and dkL/dE structures observed around L -CP of HT-GaAs is well explained by equation (1) based on the rigid band

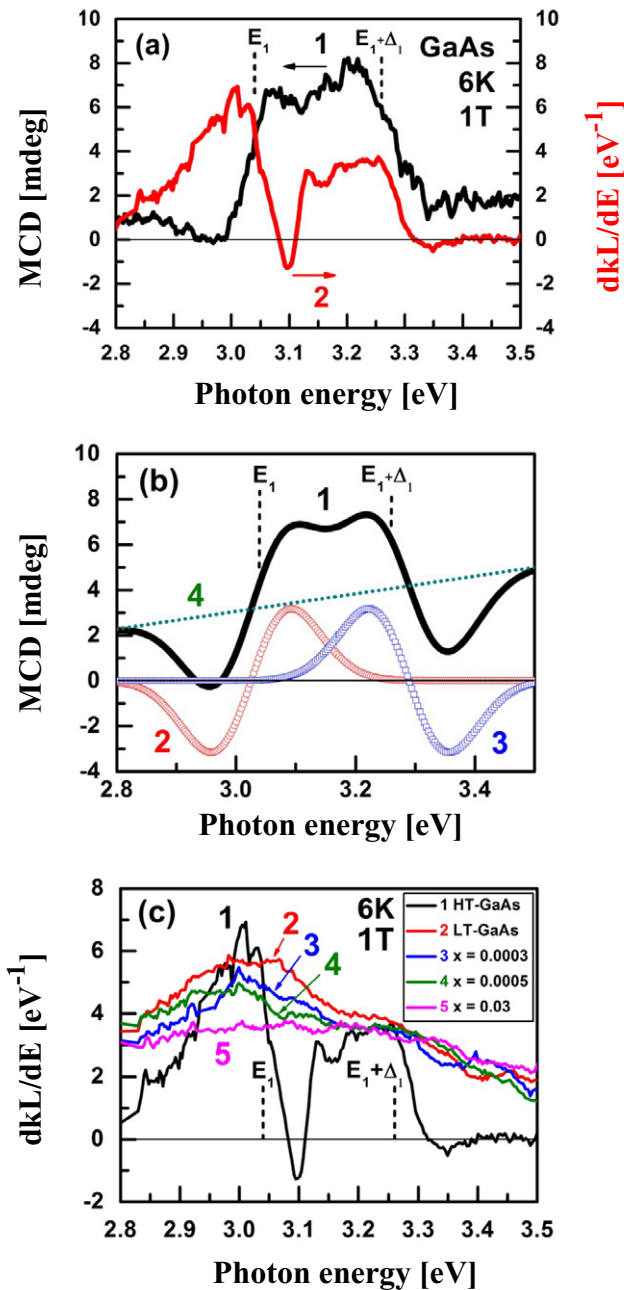


Figure 3. (a) MCD and dkL/dE spectra of HT-GaAs measured at 6 K and 1 T. Reproduced with permission from [33], Copyright 2008 American Physical Society. (b) Fitted MCD spectrum (line 1) of measured MCD spectrum is a sum of a linear background (line 4) and two dispersion curves (line 2 and 3) with same widths and same magnitudes with opposite polarities due to E_1 and $E_1 + \Delta_1$ optical transitions. (c) dkL/dE spectra of $Ga_{1-x}Mn_xAs$ with different Mn concentrations at 6 K.

shift model [22]. Figure 3(c) shows dkL/dE spectra of $Ga_{1-x}Mn_xAs$ with different Mn concentrations at 6 K. The two well-separated dkL/dE structures observed in HT-GaAs are no longer clearly observed in LT-GaAs although a shoulder around $E_1 + \Delta_1$ can be discerned. As the concentration of Mn increases, the dkL/dE spectrum becomes even broader and the shoulder starts to disappear. These broadenings originate from the inherent degradation of low temperature grown $Ga_{1-x}Mn_xAs$, as similarly observed for the MCD spectra.

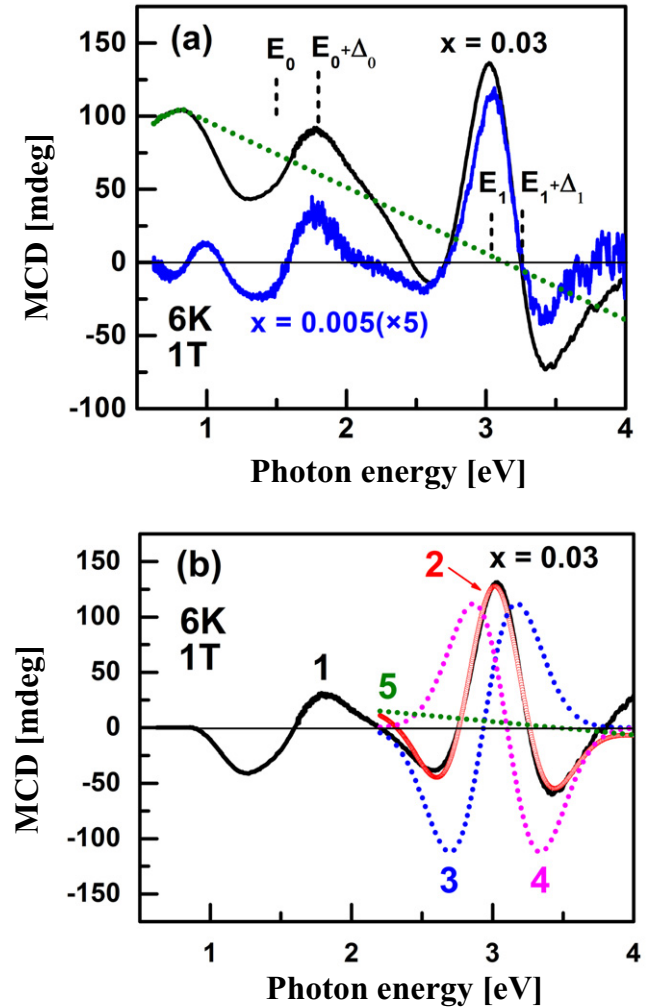


Figure 4. (a) MCD spectra of $Ga_{1-x}Mn_xAs$ with $x = 0.03$ and $x = 0.005$ (multiplied by 5). Assumed MCD linear background is shown by a green short dotted line. (b) MCD spectrum of $x = 0.03$ sample (line 1) after subtracting the background. The fitted curve (line 2) is a sum of a linear background (line 5) and two dispersion curves (line 3 and 4) with same widths and same magnitudes with opposite polarities due to E_1 and $E_1 + \Delta_1$ optical transitions.

Moreover, it can be seen in figure 3(c) that the dkL/dE spectra around L -CP do not show noticeable energy shift with increase in Mn concentration, which is in sharp contrast with the clear red-shift observed in the corresponding MCD spectra.

4. Discussions

The MCD spectrum of a $Ga_{1-x}Mn_xAs$ ($x = 0.03$) sample shows a slight kink structure around 2.2 eV (figure 4(a)). It is interesting to note that an MCD spectrum of $Ga_{1-x}Mn_xAs$ ($x = 0.05$) sample reported by Boschoten *et al* [24] also showed a very similar kink structure from 2.0 to 2.2 eV although they did not discuss its origin. To understand the origin of this structure, we first considered the MCD spectrum of $Ga_{1-x}Mn_xAs$ ($x = 0.005$) as shown in figure 4(a). A positive MCD below 2.0 eV apparently results from the $E_0 + \Delta_0$ optical transition, and a negative MCD above 2.2 eV comes from the E_1 optical transition. $Ga_{1-x}Mn_xAs$ ($x = 0.004$)

sample with 10 times larger thickness reported in [26] more clearly showed the absence of MCD signal between 2.0 and 2.2 eV. The difference between the zero MCD signal around 2.2 eV in paramagnetic $\text{Ga}_{1-x}\text{Mn}_x\text{As}$ with very small Mn concentrations (e.g. $x = 0.005$) and a large positive MCD signal around 2.2 eV in ferromagnetic $\text{Ga}_{1-x}\text{Mn}_x\text{As}$ with high Mn concentrations (e.g. $x = 0.03$) indicates that the large positive MCD around 2.2 eV comes from the IB-related optical transitions of the ferromagnetic samples. Therefore, as the first approximation, we assumed that the IB-related MCD background can be represented by a linear line which passes a positive MCD peak around 1 eV and MCD signal at 2.2 eV as illustrated by a green short dotted line in figure 4(a). Since the optical selection rule is relaxed for the IB-related optical transitions, the broad MCD spectral shape with a long tail is reasonable. After subtracting the assumed MCD background, we obtained an MCD spectrum which should be almost free from the contributions from the IB-related optical transitions (line 1 in figure 4(b)). Features of this resultant MCD spectrum of ferromagnetic $\text{Ga}_{0.97}\text{Mn}_{0.03}\text{As}$, i.e. a negative peak around E_0 , a positive peak around $E_0 + \Delta_0$, and a positive bell-shape peak accompanied with negative side peaks around L -CPs (E_1 and $E_1 + \Delta_1$), are typically observed in traditional paramagnetic II–VI DMSs with antiferromagnetic p–d exchange interaction [14, 23]. The observed MCD spectrum of ferromagnetic $\text{Ga}_{0.97}\text{Mn}_{0.03}\text{As}$ is very ordinary except for its strong and broad positive background due to the IB-related optical transitions. This observation suggests the important role of the IB for the origin of the ferromagnetism in $\text{Ga}_{1-x}\text{Mn}_x\text{As}$ [4, 7, 9, 10, 26].

According to equation (1), the MCD structure around L -CP should be explained by a superposition of two dispersion-like components originating from the two-dimensional M_1 -type Van Hove singularity of E_1 and $E_1 + \Delta_1$ optical transitions. Indeed, figure 4(b) shows that the MCD structure around L -CP is well explained by the superposition of two energy derivatives of Gaussian functions. Since E_1 and $E_1 + \Delta_1$ optical transitions are related to each other by a spin–orbit interaction, we assumed the same widths and magnitudes with opposite polarities for the two Gaussian functions. In addition to the two dispersion-like components, we needed to assume a weak linear background (line 5), which suggests that the IB-related MCD background is not so simple in a wide photon energy range as we assumed in figure 4(a). However, we believe that the essence of our following discussions will not be affected by such minor ambiguity of the weak linear MCD background.

Figure 5(a) shows energies of E_1 and $E_1 + \Delta_1$ obtained by fitting together with those of MCD peak and dkL/dE peak as a function of Mn concentration x . As already mentioned, L -CPs shift to lower energy and then start to saturate when Mn concentration is around $x = 0.001$. On the other hand, the dkL/dE peak position does not shift as Mn concentration changes. According to equation (1) which is derived based on an assumption that the spin-dependent band structure is uniform through an entire sample, MCD structures are expected to change in the same way as dkL/dE structures on the energy scale. It has been reported that Mn atoms in $\text{Ga}_{1-x}\text{Mn}_x\text{As}$ are actually inhomogeneously distributed through the sample on atomic scale and that causes

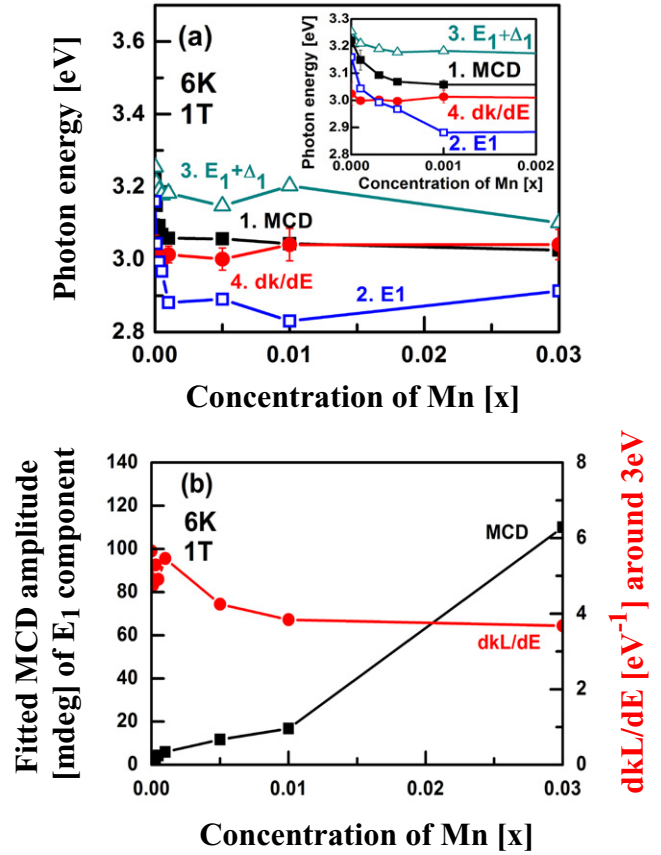


Figure 5. (a) Energies of MCD peak (1), E_1 (2), $E_1 + \Delta_1$ (3) and dkL/dE peak (4) at 6 K as a function of Mn concentration x . E_1 and $E_1 + \Delta_1$ were obtained by fitting the MCD spectral shape. Inset shows the magnification of smaller Mn concentration data. (b) Fitted MCD amplitude of the E_1 component and measured dkL/dE value around 3 eV as a function of Mn concentration x .

atomic-scale fluctuation in the local electronic density of state [35, 36]. Thus, we propose that the different behaviours of MCD and dkL/dE spectra found in this study can be explained by this microscopic inhomogeneity of electronic structure. MCD selectively detects signals from energy bands which are affected by s, p–d exchange interaction. On the other hands, dkL/dE signal captures the characteristics of the entire sample. Figure 6 shows a schematic model to explain the relation between MCD and dkL/dE of $\text{Ga}_{1-x}\text{Mn}_x\text{As}$ as a function of Mn concentration. In this model, a rigid sphere of influence exists around Mn atom, and d-electrons of Mn cause exchange interaction with s, p-electrons of GaAs host to enhance the MCD effect inside the sphere. There is no influence of d-electrons outside of the sphere, which does not cause enhancement of the MCD signal. Therefore, this model indicates the strongly localized nature of the spin-polarized band structure of $\text{Ga}_{1-x}\text{Mn}_x\text{As}$. It should be noted that the inhomogeneity discussed here is a not macroscopic one and the variation of the optical properties should be very small because the material is pure $\text{Ga}_{1-x}\text{Mn}_x\text{As}$ and is free from second-phase materials with large difference in optical properties. It means that our MCD and dkL/dE data are free from some optical interference effects observed in macroscopic inhomogeneous materials with large optical property variations.

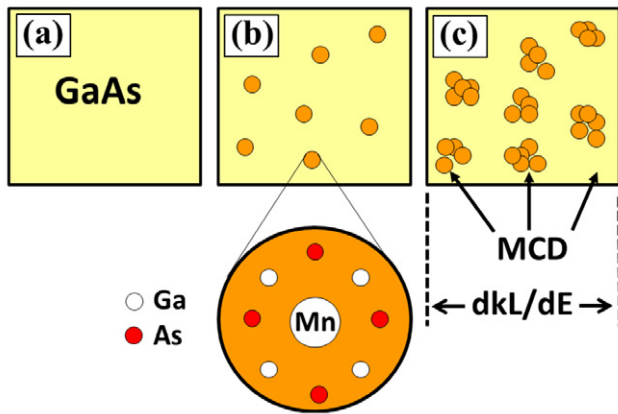


Figure 6. Empirical model to describe a relationship between MCD and dkL/dE signals for (a) pure GaAs, (b) $Ga_{1-x}Mn_xAs$ with lower Mn concentrations and (c) $Ga_{1-x}Mn_xAs$ with higher Mn concentrations.

From the decomposed MCD spectral shape (figures 3(b) and 4(b)), we tried to estimate the Zeeman splitting ΔE of the E_1 optical transition using equation (1). The estimated effective g -values of HT-GaAs using equations (1) and (2) are -1.0 and $+2.0$ for E_1 and $E_1 + \Delta_1$, respectively. These effective g -values are reasonable [33, 37] and justify the applicability of equation (1) to HT-GaAs. The fitted MCD magnitude and width of a ferromagnetic $Ga_{0.97}Mn_{0.03}As$ are 110 mdeg and 0.47 eV, respectively. These values are about 35 times larger and 3.5 times wider than those of HT-GaAs. The Mn concentration dependence of dkL/dE is much weaker than that of MCD intensity (figure 5(b)). As a value of dkL/dE for equation (1), we used half of the dkL/dE peak value around 3.0 eV because the very broadened dkL/dE spectra can be considered as a superposition of two broad spectra originating from E_1 and $E_1 + \Delta_1$ optical transitions. According to our model, schematically shown in figure 6, MCD probes only part of the sample affected by Mn atoms whereas dkL/dE probes the entire sample. In that case, the absorbance kL can be considered as $kL = k_{Mn}L_{Mn} + k_{nonMn}(L - L_{Mn})$, where k_{Mn} is the absorption coefficient, L_{Mn} is the effective length of Mn affecting area and k_{nonMn} is the absorption coefficient of non-Mn affecting area on the sample. Thus, one can expect that observed dkL/dE should be larger than the real expected value, $dk_{Mn}L_{Mn}/dE$, for the spin-polarized part of $Ga_{1-x}Mn_xAs$ if the broadening due to the low temperature growth is reasonably assumed to be uniform. Therefore, the Zeeman splitting energy that we estimate using equation (1) should be considered as the minimum limit.

By following the procedure outlined above, the evaluated Zeeman splitting energy ΔE at E_1 in $Ga_{0.97}Mn_{0.03}As$ was $+7.8$ meV. It is known that Zeeman splitting energy ΔE at E_1 of paramagnetic $Cd_{1-x}Mn_xTe$ ($x = 0.01-0.39$) at 4.5 K and 1 T is 0.5–2.0 meV [16, 17], and that of paramagnetic $Zn_{1-x}Mn_xTe$ ($x = 0.02-0.17$) is 0.5 meV [18]. In spite of its ferromagnetic nature, ΔE at E_1 of $Ga_{1-x}Mn_xAs$ ($x = 0.03$) is a little bit smaller than the reported Zeeman splitting energies in paramagnetic $Cd_{1-x}Mn_xTe$ and $Zn_{1-x}Mn_xTe$. However, the estimated ΔE value for the E_1 optical transition in

$Ga_{0.97}Mn_{0.03}As$ should be considered as the minimum limit as mentioned above.

The Zeeman splitting of ferromagnetic $Ga_{1-x}Mn_xAs$ at Γ -CPs has not been reported due to the fact that reliable analysis of MCD spectral shape around Γ -CPs is very difficult because of the strong broadening of the MCD spectra and the overlap with IB-related optical transitions [26]. Optical absorption should be also strongly deformed by the IB-related optical transitions. Still, it is worth mentioning here that the electronic states at Γ - and L -CPs of a zinc-blend structure material are not independent of each other because they are originated from the same s and p orbitals. This fact suggests that there can be some relationship between the Zeeman splitting at Γ - and L -CPs. In $Cd_{1-x}Mn_xTe$, the Zeeman splitting at E_0 is experimentally reported to be about 16 times larger than that at E_1 [17, 22, 38]. Such rapid decrease in the Zeeman splitting away from the Γ zone centre is also supported by a theory which takes into account the effect of kinetic exchange contribution to the conduction band [38, 39]. We estimated the Zeeman splitting at E_0 by multiplying the Zeeman splitting at E_1 by 16. This discussion is based on fundamental similarities of the electronic structures of $Cd_{1-x}Mn_xTe$ and $Ga_{1-x}Mn_xAs$. In $Cd_{1-x}Mn_xTe$, the energies of E_0 , E_1 , $E_1 + \Delta_1$ and $e_d^{+\sigma}$ level (Mn occupied level below top of valence band) are ~ 1.6 eV, ~ 3.4 eV, ~ 4.0 eV and 3.5 eV, respectively [13, 26, 40]. Similarly, in $Ga_{1-x}Mn_xAs$, the energies of E_0 , E_1 , $E_1 + \Delta_1$ and $e_d^{+\sigma}$ level are ~ 1.5 eV, ~ 3.0 eV, ~ 3.2 eV, and ~ 4.5 eV, respectively [26, 41]. Furthermore, the ratio of absolute value of MCD area between the Γ -CPs (1.5–2.9 eV) and the L -CPs (2.9–4.1 eV) in $Cd_{0.95}Mn_{0.05}Te$ [22] is 0.8 whereas in $Ga_{0.97}Mn_{0.03}As$ the same ratio between the Γ -CPs (0.5–2.2 eV) and the L -CPs (2.2–3.8 eV) is 0.4. Thus, the fact that the ratio of $Cd_{0.95}Mn_{0.05}Te$ and $Ga_{0.97}Mn_{0.03}As$ after subtracting the impurity-band related background is of the same order, let us believe that our estimation is correct, although such ratios do not directly relate to the relative magnitude of the observed Zeeman splitting.

Thus, the minimum limit of the Zeeman splitting of ferromagnetic $Ga_{0.97}Mn_{0.03}As$ is estimated to be $+120$ meV at E_0 . The Zeeman splitting of interband optical transition discussed here is the combination of the Zeeman splittings of the valence and conduction bands. In DMSs with zincblend structure, Zeeman splitting of the valence band is dominant over that of the conduction band due to the symmetry of s , p - d exchange interactions [14, 42]. Our result indicates a sizable Zeeman splitting of the valence band of ferromagnetic $Ga_{1-x}Mn_xAs$. Recently, electrical tunnelling spectroscopy [9] reported a very small (only several meV) Zeeman splitting of the valence band in a ferromagnetic $Ga_{1-x}Mn_xAs$ with high T_c of 154 K. In contrast, our MCD analysis shows that the Zeeman splitting at the band gap is much larger even for a sample with the lower T_c of 20 K. The reason of this discrepancy is not clear at this point.

5. Conclusions

Systematic investigations of ferromagnetic $Ga_{1-x}Mn_xAs$ show that the MCD structures at L -CPs shift to lower energy

with an increase in Mn concentration while the corresponding dkL/dE spectral structures do not show any significant change with Mn concentration. This unexpected behaviour can be explained by an empirical model indicating that MCD locally probes certain area affected by d-electrons whereas the dkL/dE spectrum results from the overall sample response. This, in turn implies that the spin-affected band structure of $Ga_{1-x}Mn_xAs$ has a strongly localized nature. The minimum value of the Zeeman splitting energy at E_1 of a ferromagnetic $Ga_{0.97}Mn_{0.03}As$ sample was estimated by the MCD spectral shape analysis. This was done after correcting for the strong background signal due to impurity band-related optical transitions. Finally, the Zeeman splitting energy at the E_0 band gap was also evaluated by assuming the same ratio between the Zeeman splitting at E_0 and E_1 observed experimentally in II–VI diluted magnetic semiconductors. The valence band of ferromagnetic $Ga_{1-x}Mn_xAs$ should have a sizeable Zeeman splitting.

Acknowledgments

WMJ and HT acknowledge support from the National Science Foundation CAREER Award No DMR-1056493, and the Condensed Matter and Surface Science (CMSS) Programme at Ohio University.

References

- [1] Ohno H, Shen A, Matsukura F, Oiwa A, Endo A, Katsumoto S and Iye Y 1996 *Appl. Phys. Lett.* **69** 363
- [2] Ohno H 1999 *Magn. Magn. Mater.* **200** 110
- [3] Lang R, Winter A, Pascher H, Krenn H, Liu X and Furdyna J K 2005 *Phys. Rev. B* **72** 024430
- [4] Burch K S, Shrekenhamer D B, Singley E J, Stephens J, Sheu B L, Kawakami R K, Schiffer P, Samarth N, Awschalom D D and Basov D N 2006 *Phys. Rev. Lett.* **97** 087208
- [5] Chakarvorty R, Zhou Y Y, Cho Y J, Liu X, Jakiela R, Barcz A, Furdyna J K and Dobrowolska M 2007 *IEEE Trans. Magn.* **43** 6
- [6] Berciu M *et al* 2009 *Phys. Rev. Lett.* **102** 247202
- [7] Ohya S, Muneta I, Hai P N and Tanaka M 2010 *Phys. Rev. Lett.* **104** 167204
- [8] Dietl T 2010 *Nature Mater.* **9** 965
- [9] Ohya S, Takata K and Tanaka M 2011 *Nature Phys.* **7** 342
- [10] Dobrowolska M., Tivakornsasithorn K, Liu X, Furdyna J K, Berciu M, Yu K M and Walukiewicz W 2012 *Nature Mater.* **11** 444
- [11] Ohya S, Muneta I, Xin Y, Takata K and Tanaka M 2012 *Phys. Rev. B* **86** 094418
- [12] Chapler B C *et al* 2012 *Phys. Rev. B* **86** 165302
- [13] Furdyna J K 1988 *J. Appl. Phys.* **64** R29
- [14] Ando K 2000 *Magneto-Optics (Springer-Verlag Series in Solid-State Science vol 128)* ed S Sugano and N Kojima (Berlin: Springer) pp 211–44
- [15] Ando K 2006 *Science* **312** 1883
- [16] Ginter J, Gaj J A and Dang L S 1983 *Solid State Commun.* **48** 849
- [17] Coquillat D, Lascaray J P, Desjardins-Deruelle M C, Gaj J A and Triboulet R 1986 *Solid State Commun.* **59** 25
- [18] Coquillat D, Lascaray J P, Gaj J A, Deportes J and Furdyna J K 1989 *Phys. Rev. B* **39** 88
- [19] Ando K and Akinaga H 1995 *Magn. Magn. Mater.* **104** 2029
- [20] Saito H, Zayets V, Yamagata S and Ando K 2002 *Phys. Rev. B* **66** 081201
- [21] Saito H, Zayets V, Yamagata S and Ando K 2003 *Phys. Rev. Lett.* **90** 207202
- [22] Ando K, Saito H and Zayets V 2011 *J. Appl. Phys.* **109** 07C304
- [23] Ando K, Hayashi T, Tanaka M and Twardowski A 1998 *J. Appl. Phys.* **83** 6548
- [24] Beschoten B, Crowell P A, Malajovich I and Awschalom D D 1999 *Phys. Rev. Lett.* **83** 3073
- [25] Chakarvorty R, Shen S, Yee K J, Wojtowicz T, Jakiela R, Barcz A, Liu X, Furdyna J K and Dobrowolska M 2007 *Appl. Phys. Lett.* **91** 171118
- [26] Ando K, Saito H, Agarwal K C, Debnath M C and Zayets V 2008 *Phys. Rev. Lett.* **100** 067204
- [27] Ando K 2009 *Appl. Phys. Lett.* **94** 156101
- [28] Ando K, Saito H, Agarwal K, Debnath M and Zayets V 2009 *Phys. Rev. Lett.* **102** 069702
- [29] Szczytko J, Mac W and Twardowski A 1999 *Phys. Rev. B* **59** 935
- [30] Becquerel H 1897 *C. R. Acad. Sci.* **125** 679
- [31] Cardona M 1969 *Modulation Spectroscopy Solid State Physics Supplement 11* (New York: Academic)
- [32] Aspnes D E and Studna A A 1973 *Phys. Rev. B* **7** 4605
- [33] Ando K, Saito H, Debnath M C and Zayets V Bhattacharjee A K 2008 *Phys. Rev. B* **77** 125123
- [34] Yu P Y and Cardona M 2000 *Fundamentals of Semiconductors Physics and Materials Properties* 4th edn (Berlin: Springer) pp 261–8
- [35] Mahieu G, Condet P, Grandidier B, Nys J P, Allan G, Stievenard D, Ebert P, Shimizu H and Tanaka M 2003 *Appl. Phys. Lett.* **82** 712
- [36] Richardella A, Roushan P, Mack S, Zhou B, Huse D A, Awschalom D D and Yazdani A 2010 *Science* **327** 665
- [37] Fujimori A, Fukutani H and Kuwabara G 1978 *J. Phys. Soc. Japan.* **45** 910
- [38] Bhattacharjee A K 1990 *Phys. Rev. B* **41** 5696
- [39] Bhattacharjee A K and Perez-Conde J 2000 *Proc. 25th Int. Conf. on Physics of Semiconductors (Osaka, Japan)* ed N Miura and T Ando p 242
- [40] Zimmnal-Starnawska M, Podgorny M, Kisiel A, Giriat W, Demianiuk M and Zmija J 1984 *J. Phys. C Solid State Phys.* **17** 615
- [41] Okabayashi J, Kimura A, Mizokawa T, Fujimori A, Hayashi T and Tanaka M 1999 *Phys. Rev. B* **59** R2486
- [42] Bhattacharjee A K, Fishman G and Coqblin B 1983 *Physica B* **117/118** 449